Available online at www.sciencedirect.com
SCIENCE DIRECT®
International Journal of Thermal Sciences 44 (2005) 1–10
International Journal of Thermal Sciences
www.elsevier.com/locate/ijts

Solutal-thermo-diffusion convection in a vibrating rectangular cavity

M. Chacha [a], M.Z. Saghir [b,*]

[a] *UAE University, Department of Mechanical Engineering, PO Box 17555 Al Ain, AD, United Arab Emirates*
[b] *Ryerson University, Department of Mechanical Engineering, 350 Victoria Street, Toronto, ON, M5B 2K3 Canada*

Received 16 December 2003; received in revised form 23 April 2004; accepted 23 April 2004

Available online 15 July 2004

Abstract

Diffusion-dominated experiments on-board the International Space Station and other free-flying platforms are affected by the convective flow due to the residual acceleration field and/or to the oscillatory accelerations (g-jitters) caused by several external sources. We are interested in investigating these effects on the solutal-thermo-diffusion for a binary fluid mixture. We considered a rectangular rigid cavity filled with methane (20%) and normal butane (80%), subject to a temperature difference on its lateral walls and radiation heat transfer on the horizontal walls. The full transient Navier–Stokes equations, accounting for a unique mode of oscillatory acceleration, coupled with the mass and heat transfer formulations and the equation of state of the fluid were solved numerically using the control volume technique. The species transport equation accounts for varying diffusion coefficients with the temperature and the fluid composition and their effect is analysed as compared to that of their average constant values. Results revealed that convection is enhanced and temperature and species profiles distortion from purely diffusive (zero-gravity) condition increases in a buoyancy-destabilizing configuration. The numerical study shows that by elimination both the residual gravity and the g-jitter levels are essential to achieve nearly purely diffusive conditions when their direction is orthogonal to that of the temperature gradient. For the configuration investigated, the g-jitter is found to reduce compositional variation. When quasi-steady state conditions are attained, thermal and compositional quantities fluctuate following a mode whose fundamental (primary) frequency is equal to that of the initially imposed vibration.
© 2004 Elsevier SAS. All rights reserved.

Keywords: Convection; Soret effect; Micro-gravity; g-jitter; Control volume method

1. Introduction

Thermal diffusion—Soret effect—causes a composition gradient to arise in an initially homogeneous mixture due to the temperature gradient. This effect can be quite important in the analysis of compositional variation in hydrocarbon reservoirs. Great efforts have been invested in the development of theoretical models as well as experimental set-ups to account for and quantity the importance of this effect in reservoir modelling in order to enhance oil recovery. Because of buoyancy-induced convection in the gravitational field, accurate measurement of the Soret coefficient for multi-component mixtures is nearly impossible. Even when one had succeeded to 'eliminate' gravity-induced convection in ground-based experiments, results have revealed up to 50% discrepancy. Therefore an emergence of conducting experiments in micro-gravity environment is important to set benchmarks and help refining ground-based procedures. Analysis of the effective acceleration environment from space missions has shown that the acceleration field contains a constant component (residual-gravity) and oscillatory components (g-jitters) covering a wide spectrum of amplitudes and frequencies. The g-jitters effects on space experiments are largely unknown. Considering the contribution of the g-jitters and residual-gravity in theoretical and numerical models thus appears detrimental for a better understanding and analysis of the diffusion measurement from experiments carried out on free-flying platforms where buoyancy is minimized.

Free convection is driven by buoyancy forces, which result from both density gradients and gravity field. When a system with density gradients is subject to vibrations, the resulting buoyancy forces produced by the interaction of the density gradients with the acceleration field have a complex spatial and temporal structure depending on both the nature of the density gradients and the spatial and frequency

* Corresponding author.
E-mail address: zsaghir@ryerson.ca (M.Z. Saghir).

1290-0729/$ – see front matter © 2004 Elsevier SAS. All rights reserved.
doi:10.1016/j.ijthermalsci.2004.04.013

Nomenclature

a	interaction energy between molecules	$\mathrm{J{\cdot}m^3{\cdot}mol^{-2}}$	
b	hard-core or co-volume parameter	$\mathrm{m^3{\cdot}mol^{-1}}$	
c	transported component mass fraction		
c_0	initial butane mass fraction		
c_p	mixture specific heat at constant pressure	$\mathrm{J{\cdot}kg^{-1}{\cdot}K^{-1}}$	
D^c	mass diffusivity	$\mathrm{m^2{\cdot}s^{-1}}$	
D^T	thermal diffusion coefficient	$\mathrm{m^2{\cdot}s^{-1}{\cdot}K^{-1}}$	
f	frequency of the g-jitter	Hz	
g	magnitude of acceleration due to gravity	$\mathrm{m{\cdot}s^{-2}}$	
g_0	earth gravity acceleration magnitude, $= 9.81\ \mathrm{m{\cdot}s^{-2}}$		
g_1	magnitude of the (quasi)-static gravity	$\mathrm{m{\cdot}s^{-2}}$	
g_2	amplitude of the g-jitter	$\mathrm{m{\cdot}s^{-2}}$	
k	mixture thermal conductivity	$\mathrm{W{\cdot}m^{-1}{\cdot}K^{-1}}$	
L	cavity length	mm	
H	cavity height	mm	
p	pressure	Pa	
p_{T_m}	pressure at mean temperature	Pa	
R	universal gas constant, $8.31441\ \mathrm{J{\cdot}mol^{-1}{\cdot}K^{-1}}$		
S^T	Soret coefficient	$\mathrm{K^{-1}}$	
t	time	s	
T	temperature	K	
T_0	room/initial temperature	K	
T_c	cold wall temperature	K	
T_h	hot wall temperature	K	
T_m	mean temperature	K	
T_∞	temperature of the surroundings	K	
u	velocity component in x-direction	$\mathrm{m{\cdot}s^{-1}}$	
v	velocity component in y-direction	$\mathrm{m{\cdot}s^{-1}}$	
$\tilde{v}$	mixture molar volume	$\mathrm{m^3{\cdot}mole^{-1}}$	
(x, y)	Cartesian coordinates	m	

Greek symbols

ε	emissivity of the radiating walls	
μ	mixture dynamic viscosity	Pa·s
ω	pulsation of the g-jitter, $= 2\pi f$	$\mathrm{rad{\cdot}s^{-1}}$
ρ	mixture mass density	$\mathrm{kg{\cdot}m^{-3}}$
σ	Stefan–Boltzmann constant, $5.67032\ \mathrm{W{\cdot}m^{-2}{\cdot}K^{-4}}$	

distribution of the vibration-induced acceleration field. The g-jitter environment is being characterized in a growing literature. Theoretical work on the instability in fluids under the influence of g-jitter in weightlessness conditions has been reported by Merkin [1], Davidson [2] and Haddon and Riley [3]. Their results revealed that convection induced by g-jitter resulted in a significant increase of the heat transport when compared with the purely diffusive distribution. Rees and Pop [4,5] studied the influence of periodical gravity modulation on free convection in porous media. They determined the detailed effect of the g-jitter' amplitude and frequency on the flow and heat transfer characteristics. In [4], they showed how the boundary-layer flow induced by a constant temperature vertical surface embedded in a fluid-saturated porous medium is modified by time-periodic variations in the gravitational acceleration using a small amplitude expansion up to fourth-order. An asymptotic analysis showed that the g-jitter effect is eventually confined to a thin layer embedded within the main boundary-layer, and becomes weak at increasing distances from the leading edge. In [5], they examined the response of a nonlinear system consisting of a flow near the front stagnation of a cylindrical surface with a constant temperature to a time-periodic perturbation of the gravitational field. It was found that low-frequency g-jitter has a significant effect on the stability of the system. For large values of the forcing frequency, the numerical evidence seemed to suggest that the flow is unaffected by g-jitter effect at leading order, while at small values of the frequency, the heat transfer response is almost exactly in phase with the gravitational acceleration. The effect of increasing the values of the forcing amplitude is to give an almost proportional increase in the shear stress and rate of heat transfer responses, so long as the Prandtl number is kept constant. They noticed a persistence of the velocity and temperature oscillations even when the thermal field was conductive and concluded that this could be of importance in mass transport processes in the presence of impurities. Jue and Ramaswamy [6] studied a two-dimensional thermosolutal convection flow (with no Soret effect) under a sinusoidal gravity modulation field. The fingering regime (regime set with a destabilizing solute field and a stabilizing thermal field) and the diffusive regime (destabilizing thermal field) were explored for a series of gravity modulation frequencies. Two types of flow evolution, synchronous and subharmonic responses, were obtained for different frequencies. They showed that the increase in gravity modulation frequency provides larger heat and mass transfer rates in the fingering regime; but results in smaller value in the diffusive regime.

In a new approach to g-level tolerability for fluid and material science experiments, Monti and Savino [7] carried out the analysis of the general case of quasi steady residual g-levels superimposed to high frequency-small amplitude g-disturbances by means of a time-averaged formulation. This helps in evaluating the maximum allowable g-levels of high frequencies periodic disturbances that specific micro-gravity experiments can tolerate. They numerically analyzed the thermo-fluid-dynamic distortions as function of the classical Rayleigh number for steady g, and of the vibrational Rayleigh number, for high frequencies g-jitters. On the basis of their results, the g-tolerability domain was drawn for a study case on thermal diffusion in a fluid cell. Savino et

al. [8] performed a three-dimensional numerical simulation on a fluid cell subject to periodic accelerations of relatively high frequencies, i.e., $f \geqslant 1$ Hz, orthogonal to the density gradient. The attention was focused on the time averaged convective motion arising from thermo-vibrational effects. The 3D numerical results presented in terms of velocity and temperature fields enable to evaluate the range of validity of the two-dimensional assumption routinely invoked. Globally, the results show that the vector plots and the isotherms in the mid-section of the cell $z = A/2$ are qualitatively similar to the analogous 2D fields ($A = L_z/L$ is the aspect ratio of the cell of dimensions $L \times L \times L_z$). However quantitatively, significant differences between 2D and 3D results exist for small values of the aspect ratio because of the influence of the viscous side wall effects. The 3D results approach those obtained under 2D assumption when the aspect ratio increases. Larger value of the aspect ratio A is necessary at large Rayleigh numbers to obtain a good description of the field in the mid-section $z = A/2$ using a 2D formulation as the influence of the side walls increases with the vibrational Rayleigh number.

Reducing the gravity field reduces the Fickian diffusivity value as compared to that obtained at g_0-level and the reduction of g-jitter afforded on-board free-flying platforms reduces the measured value of the Fick diffusion coefficient even further; see Smith et al. [9]. Savino and Monti [10] studied the natural and vibrational convection induced by steady residual-g and high frequency g-jitters in a typical process for the measurement of the diffusion coefficients in liquids at isothermal conditions (Fick diffusion) onboard the orbiting platforms. They demonstrated through numerical experiments that a residual-g of the order of magnitude of $10^{-6}g_0$ is responsible for a negligible error in the measurement of the Fick diffusion coefficient, whereas more relevant distortions could be associated to extremely large g-jitters.

The preceding studies showed that convection in microgravity environment is related to the magnitude of g-jitter and to the alignment of the gravity field with respect to the growth or the direction of the temperature gradient. It was found that the frequency, amplitude and spatial orientation of the residual gravity vector all play an important role in determining the convective flow behaviour of the system. However, such research was focused on the onset of natural convection and only a few authors included the Fick diffusion in their analysis as in [10]. Very limited efforts have been directed towards the study of g-jitter effects in double-diffusion situations, i.e., vibrational convection of a fluid mixture in the presence of Soret effect. In their pioneering work, Gershuni et al. [11] investigated theoretically the linear stability of a plane horizontal layer of a binary mixture with Soret effect subject to a static gravity and longitudinal high-frequency vibration. The study was based on the closed system of equations, obtained by applying the averaging technique to describe the behaviour of the mean field. This resulted in the derivation of the convection stability limits and provided qualitative understandings of different instability mechanisms and forms. Later on, Gershuni et al. [12] studied the stability of the mechanical equilibrium of a plane horizontal binary mixture layer with Soret effect in the presence of high frequency transversal vibration. They showed from the asymptotic analysis for long-wave disturbances and from the numerical solution of the spectral amplitude problem for cellular disturbance that independently of the properties of the binary mixture, the effect of the transversal vibration is always stabilizing. Studying the convective disturbances induced by g-jitters on the space station, Monti et al. [13] demonstrated that under the assumption of small amplitudes and large frequencies of the oscillatory accelerations, direct numerical solution of the full Navier–Stokes equations containing time-dependent accelerations yields similar results as those obtained solving the time-averaged field equations (Gershuni's formulation), containing all the g-jitter terms grouped in a single parameter. Considering a typical experiment with metal alloys the difference between direct and time-averaged formulations was found to be less than 1%. They showed that while no separation occurs on earth in this particular system, separation does take place in microgravity environment rendering Soret coefficient measurement feasible; and the apparent value obtained in the presence of residual-g and g-jitter could be up to 30% smaller than the real one. Results obtained by Savino [14] show that for the microgravity level on board the International Space station, the two formulations give almost the same results and orienting the residual-g parallel to the density gradient, reduces the convective disturbances and can also help mitigating the disturbances induced by the g-jitter.

Chacha et al. [15] studied the solutal thermodiffusion in a binary mixture subject to the influence of residual gravity field and (single mode) moderately high frequency g-jitter acceleration under Boussinesq approximation, using the finite-element method. For the different configurations investigated, the g-jitter was found to reduce compositional variation and synchronous responses of the flow evolution were obtained.

In this paper we study the effect of vertical g-jitter and residual gravity on mass-thermo-fluid dynamics in a fluid mixture by performing a direct numerical simulation of the time-varying processes using the control volume method. We consider a finite two-dimensional binary mixture of methane and n-butane (C_1/nC_4) subject to lateral temperature gradient including the Soret effect under the influence of vibrational instability in micro-gravity environment. The mathematical formulation of the problem in dimensional form is introduced in Section 2. Our mathematical model accounts for the fluid density variation as well as the variation of species diffusion (Fick diffusion) and thermal diffusion (Soret diffusion) coefficients with the temperature and the fluid composition. Section 3 presents the numerical procedure adopted for the problem solution. In Section 4 we discuss the results obtained for different micro-gravity conditions and the effects of varying transport coefficients. Section 5 concludes the results of this work.

2. Problem description and basic equations

In this section, we describe the basic equations, boundary and initial conditions that govern the problem. The physical model of the cavity under study is sketched in Fig. 1. The system consists of a rectangular cavity ($H \times L$) containing a single-phase binary fluid mixture in micro-gravity environment under the influence of residual gravity. The cavity may be subject to vibrational effects due to oscillatory acceleration component called g-jitter. The cavity vibration is modelled by a harmonic contribution to the body force. Both the residual gravity and the g-jitter are assumed to be perpendicular to the thermal gradient. The cavity is allowed to exchange heat with its environment at T_∞ through radiation process at its horizontal walls. The vertical walls are set to constant temperatures, T_h and T_c with T_h greater than T_c (horizontal thermal gradient). All walls are assumed to be rigid and impermeable to matter.

2.1. Mass conservation equation

The principle of mass conservation applied to the fluid mixture accounting for the variation of the density results in the following equation:

$$\frac{\partial \rho}{\partial t} + \frac{\partial \rho u}{\partial x} + \frac{\partial \rho v}{\partial y} = 0 \tag{1}$$

For the solute and in terms of its mass fraction c, the principle of mass conservation results in:

$$\begin{aligned}\frac{\partial}{\partial t}(\rho c) + \frac{\partial}{\partial x}(\rho u c) + \frac{\partial}{\partial y}(\rho v c) &= \frac{\partial}{\partial x}\left[\rho\left(D^c \frac{\partial c}{\partial x} + D^T \frac{\partial T}{\partial x}\right)\right] \\ &\quad + \frac{\partial}{\partial y}\left[\rho\left(D^c \frac{\partial c}{\partial y} + D^T \frac{\partial T}{\partial y}\right)\right]\end{aligned} \tag{2}$$

The second component (carrier-fluid) concentration is $1 - c$. The Fickian and Soret diffusivities (D^c and D^T) are the very essential parameters for the process under investigation. They are assumed to vary with the actual local temperature, pressure and composition and can be mathematically formulated using the thermodynamics of irreversible processes as discussed in de Groot and Mazur [16], Shukla and Firrozabadi [17] and Firoozabadi [18]. Firoozabadi [18] provides the detailed analytical models for the calculation of the diffusion coefficients.

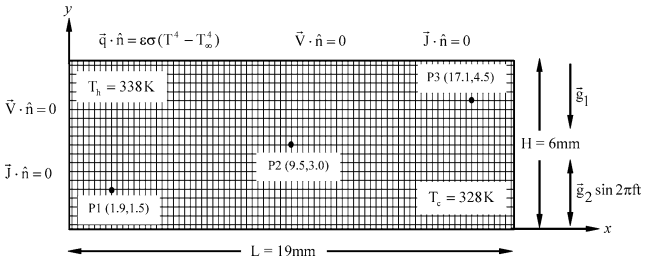

Fig. 1. Geometrical model and boundary conditions.

2.2. Momentum conservation equation

The principle of momentum conservation is represented by the Navier–Stokes equations for a weakly compressible (temperature and species varying density) fluid. In the x-direction, this equation writes

$$\begin{aligned}\frac{\partial}{\partial t}(\rho u) + \frac{\partial}{\partial x}(\rho u u) + \frac{\partial}{\partial y}(\rho v u) &= -\frac{\partial p}{\partial x} + \frac{\partial}{\partial x}\left[\mu\left(\frac{\partial u}{\partial x}\right)\right] + \frac{\partial}{\partial y}\left[\mu\left(\frac{\partial u}{\partial y}\right)\right]\end{aligned} \tag{3}$$

whereas in the y-direction, the equation is

$$\begin{aligned}\frac{\partial}{\partial t}(\rho v) + \frac{\partial}{\partial x}(\rho u v) + \frac{\partial}{\partial y}(\rho v v) &= -\frac{\partial p}{\partial y} + \frac{\partial}{\partial x}\left[\mu\left(\frac{\partial v}{\partial x}\right)\right] + \frac{\partial}{\partial y}\left[\mu\left(\frac{\partial v}{\partial y}\right)\right] + \rho g_y\end{aligned} \tag{4}$$

$$g_y = -g_1 - g_2 \sin(2\pi f t) \tag{5}$$

g_1 and g_2 are respectively the magnitude of the residual-(static) gravity and the amplitude of oscillation of the g-jitter, while f is the frequency of oscillation. The dynamic viscosity μ is assumed to be varying in the cavity as a function of the local pressure, temperature and composition. The dynamic viscosity model is found in Jossi et al. [19] as well as in Lohrenz et al. [20].

2.3. Energy conservation equation

Assuming there is no internal heat generation, the principle of conservation of energy is expressed by the following equation:

$$\begin{aligned}\frac{\partial}{\partial t}(\rho T) + \frac{\partial}{\partial x}(\rho u T) + \frac{\partial}{\partial y}(\rho v T) &= \frac{\partial}{\partial x}\left[\frac{k}{c_p}\left(\frac{\partial T}{\partial x}\right)\right] + \frac{\partial}{\partial y}\left[\frac{k}{c_p}\left(\frac{\partial T}{\partial y}\right)\right]\end{aligned} \tag{6}$$

The specific heat at constant pressure c_p and the thermal conductivity k are assumed to be constant.

2.4. Equation of state

It is necessary to define the relationship of the density of the fluid to the flow parameters such as temperature, pressure, and species concentration in order to make use of the preceding conservation equations. The Peng–Robinson equation of state (PR-EOS) [21] is adopted in the present work:

$$p = \frac{RT}{\tilde{v} - b} - \frac{a}{\tilde{v}^2 + 2b\tilde{v} - b^2} \tag{7}$$

The PR-EOS enjoys practically the same level of complexity and accuracy for phase-behavior prediction as many other cubic equations of state (SRK-EOS, etc.). Our choice was mostly a matter of simplicity and straightforwardness as the analytical models for the calculation of the mass and

thermal diffusion coefficients are derived using the PR-EOS [18]. The different steps involved in the calculation of the fluid mixture density are detailed in Chacha et al. [15]. The state of the fluid (liquid state) is fixed by the initial composition, temperature and pressure level. Pressure negligible variations in the cavity do not affect the density very much afterward. The main parameter governing the density variation in the process is the temperature variation; of a lesser but not negligible importance is the mixture compositional variation.

2.5. Boundary and initial conditions

The no flow and no-slip boundary conditions ($\vec{V}\cdot\hat{n}=0$; where $\vec{V}$ is the velocity vector and $\hat{n}$ is the outward unit vector normal to the boundary) are considered on the four walls of the rectangular cavity which are not subject to surface reactions nor to mass flux ($\vec{J}\cdot\hat{n}=0$; where $\vec{J}$ is the diffusion flux). The left vertical wall is imposed a constant temperature T_h while the right vertical wall is at T_c ($T_\mathrm{h}-T_\mathrm{c}=10$ K). The top and the bottom walls are allowed to exchange heat through radiation with the environment whose temperature is assumed to be equal to $T_\infty=303$ K ($\vec{q}\cdot\hat{n}=\Phi$; $\vec{q}$ is the conductive heat flux and Φ is the net radiation heat exchange between the sample and its surroundings). The imposed boundary conditions are shown in the physical model, see Fig. 1. For the initial conditions, the velocities in the computational domain are set equal to zero, the concentration is set equal to the initial concentration c_0, the pressure at p_{T_m} for the average temperature T_m. Initial field temperature is equal to T_0.

3. Numerical procedure

All physical properties, except the fluid thermal conductivity and specific heat at constant pressure, are varying in time and space. Table 1 lists the average working conditions, the thermo-physical properties obtained at those conditions as well as the geometric data of the system used in the numerical analysis. The average working conditions are such that the pressure at mean temperature is $p_{T_\mathrm{m}}=35$ MPa as discussed by Georis et al. [22] where $T_\mathrm{m}=\frac{1}{2}(T_\mathrm{h}+T_\mathrm{c})=333$ K.

Table 1
Average physical property of the mixture and physical model data

P_{T_m}	35 MPa	T_m	333 K
ρ	538 kg·m^{-3}	c_butane	0.8
μ	2×10^{-4} kg·m^{-1}·s^{-1}	T_c	328 K
c_p	2040 J·kg^{-1}·K^{-1}	T_h	338 K
k	0.095 W·m^{-1}·K^{-1}	T_∞	303 K
D^c	3.771×10^{-9} m^2·s^{-1}	ε	0.1
D^T	5.060×10^{-12} m^2·s^{-1}·K^{-1}	L	19 mm
$S^T=D^T/D^c$	1.342×10^{-3} K^{-1}	H	6 mm

To complete the numerical model, a pressure-correction equation is implemented. The equation for the pressure-correction inside the cavity is:

$$\frac{\partial\rho}{\partial t}+\frac{\partial}{\partial x}(\rho u^*)+\frac{\partial}{\partial y}(\rho v^*) = \frac{\partial}{\partial x}\left[\rho K_x\left(\frac{\partial p'}{\partial x}\right)\right]+\frac{\partial}{\partial y}\left[\rho K_y\left(\frac{\partial p'}{\partial y}\right)\right] \tag{8}$$

and the field pressure p is given by

$$p=p^*+p' \tag{9}$$

The exact velocity field represented by u and v is obtained by introducing the responses to the pressure corrections:

$$u=u^*-K_x\frac{\partial p'}{\partial x} \tag{10}$$

$$v=v^*-K_y\frac{\partial p'}{\partial y} \tag{11}$$

u^* and v^* are the solutions of the momentum equations corresponding to the guessed pressure field p^* and p' is the pressure correction. K_x and K_y are coefficients resulting from the discretization scheme.

The numerical procedure is based on the SIMPLE algorithm, see Patankar [23]. The NSPCG package (with MIC3 as pre-conditioner and BCGS as accelerator) was used to solve the (nonsymmetric) algebraic system of equations in u, v, p', T, and c, which resulted from the control volume approximation. The problem is strongly coupled and nonlinear since the density and the diffusion coefficients are related to the temperature, pressure and mixture composition. The convergence is achieved at each time step once the maximum of the average relative errors in the unknowns u, v, p, c and T between two successive iterations is less than 1×10^{-6}; i.e., $\mathrm{Max}(\phi_u,\phi_v,\phi_T,\phi_c,\phi_p)<10^{-6}$. The average relative error is defined by

$$\phi_F=\frac{1}{(n\times m)}\sum_{i=1}^{i=m}\sum_{j=1}^{j=n}\left|\left(F_{i,j}^{k,s+1}-F_{i,j}^{k,s}\right)/F_{i,j}^{k,s+1}\right| \tag{12}$$

where F stands for the unknown u, v, p, T or c. k denotes the time step number, while the iteration number is s. The grid point is specified by its mesh coordinates (i, j).

The time step is in general different from one study case to another as it depends strongly on the period of the imposed vibration, if any.

The Soret and Fick diffusion coefficients and the viscosity are calculated at each mesh point and are continually updated during the course of the solution procedure. Following the initial flow field described by the initial conditions, the time integration is performed using a first-order semi-implicit scheme. Time integration is pursued until the steady state is attained, when it exists. The conservation of the butane total mass fraction is satisfied at each time step. Detailed calculation steps may be found in Chacha et al. [24].

Fig. 1 shows the rectangular mesh that was used to obtain all the results reported in this paper which consist of 79 control volumes in the x-direction and 19 control volumes in the y-direction, for a total of 1701 (21×81) nodes. The locations of interest (i.e., P1, P2 and P3) in the resulting analysis are also shown in the same figure. Mesh sensitivity performed by Chacha et al. [24] revealed that the adopted mesh is accurate.

4. Results and discussion

Different acceleration levels applied to the cavity will be discussed in this section; as we will investigate the cavity under earth gravity condition, residual-gravity and micro-vibrations.

4.1. Cavity under earth gravity condition

In the case of earth gravity condition, Fig. 2 presents the convection in the cavity as well as the heat and mass transfer. As shown in Fig. 2(a), a single -boundary layer type flow- clockwise rotating convective cell is present. Because we are in the condition of side heating, the system is always unstable and no critical Rayleigh number exists. Fig. 2(b) presents the temperature distribution in the cavity. Because the horizontal walls of the cavity are subject to heat losses by radiation, nonlinear temperature distribution is obtained in the cavity. Large temperature gradient does exist at the cold and at the hot walls. This is evident from the temperature distribution shown in Fig. 2(b). During this computation, the initial temperature in the cavity was set to be the average temperature between the cold and the hot walls and the species and thermal diffusion were varying with the temperature and the fluid composition. This large mixing which is due to the buoyancy force shadowed the Soret effect and as shown in Fig. 2(c), a uniform constant distribution of the butane is found in the interior part of the cavity.

Having large temperature gradient at the two vertical walls also reflects the large mass gradient at the hot and the cold walls. The temperature profile is almost linear within the boundary layer, see Fig. 2(b). As shown in Fig. 2(c), near the hot and cold walls, important Soret effect is present which will then reduce to zero far from the lateral walls due to the strong mixing condition. Because gravity induced convection makes the measurement of the species and thermal diffusion nearly impossible to achieve in earth gravity as shown in Fig. 2, it is necessary to measure those coefficients under microgravity conditions. Preceding observations imply that ground experiments would accommodate only with very thin one-dimensional cell while microgravity experiments appear to yield more flexibility and accuracy.

In order to show the importance of adopting a variable diffusion coefficients model in time and space, Fig. 3(a) presents the case of the butane concentration distribution

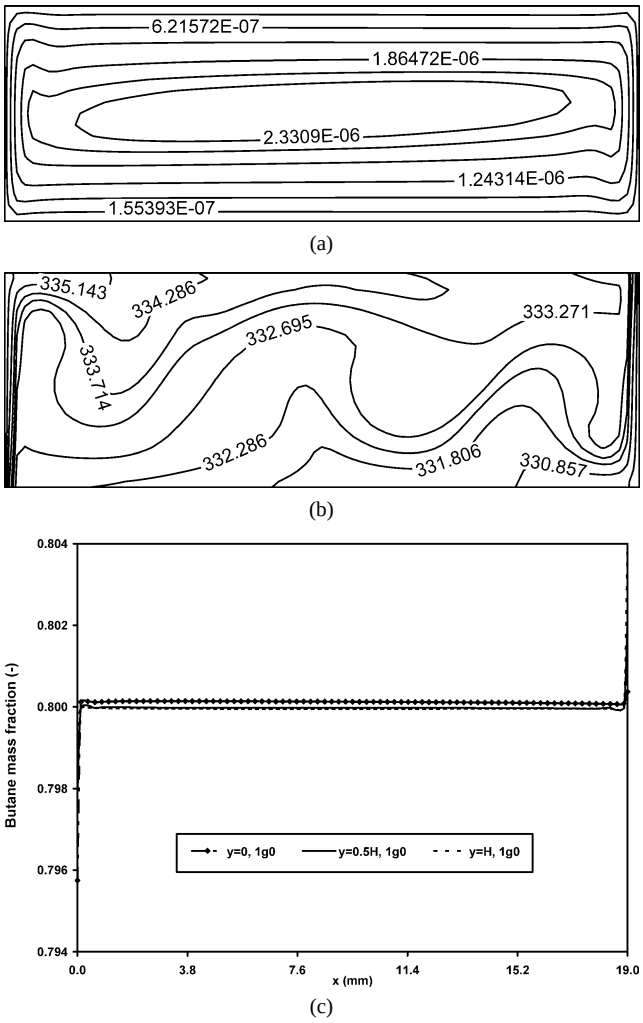

Fig. 2. Streamlines, temperature and butane distribution in the cavity. (a) Streamline; (b) Temperature contours; (c) Butane distribution.

in the cavity when the thermal and species diffusion coefficients were varying with the temperature and the fluid composition and when they were set constant. As seen in Fig. 3, the absence of gravity annihilates the mixing in the fluid cavity and, leads to a symmetric distribution of butane with respect to the horizontal centre-line. The dashed lines represent the case when the coefficients are maintained constant and the continuous lines represent the case when those coefficients are varying as functions of the temperature and the composition. Butane, which is the heavier component, migrates to the cold wall. This migration is however less pronounced—weaker—near the cold wall when the coefficients are kept constant. This reflects the importance of having the diffusion coefficients to vary in the numerical calculation rather than assuming a constant parameter. The nonlinear complex variation of the butane near the cold wall is mainly due to the nonlinear temperature distribution at the horizontal walls of the cavity; indeed because of the radiation, the 'coldest point' is situated not on the cold wall, but in an inner zone of the cavity. All other computations were done assuming a variable Soret and Fickian diffusivi-

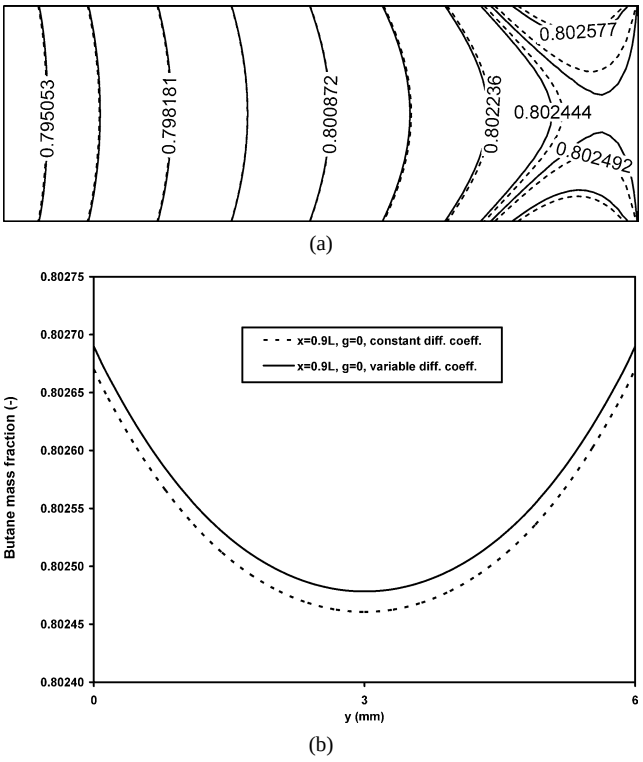

Fig. 3. Butane distributions in the cavity (- - - constant D^c and D^T, — variable D^c and D^T). (a) Butane variation in the cavity; (b) Butane variation near the cold wall.

ties. Fig. 3(b) shows the butane variation near the cold wall for the two diffusion coefficient conditions. It is clearly evident to observe a large difference in the butane variation.

4.2. Influence of the residual gravity

We have seen in the first case that gravity causes the mixing in the fluid cavity leading to a uniform mass distribution of the butane. Fig. 4 presents the case of the mass diffusion when a residual-gravity vector of 1 μg ($10^{-6}g_0$) and of 10 μg magnitude is present. Fig. 4(a) shows a comparison between the zero gravity case and a 1 μg gravity condition. The dashed line presents the mass transfer in 1 μg whereas the continuous line is for the ideal condition of zero gravity. It is evident to notice that a small residual gravity will initiate a mixing in the cavity. Such finding is more pronounced for a residual-gravity of 10 μg as shown in Fig. 4(b). Rotating flow initiates a nonuniform mass transfer variation in the computational domain. One can also notice that even with such low residual gravity, buoyancy starts to affect the mass diffusion as less butane is migrating toward the cold end of the cavity. Such finding justifies the importance of zero gravity environments to study the diffusion of different fluid mixtures. Fig. 4(c) presents the butane distribution in the vertical direction, at the middle of the cavity, for different gravity levels. In the case of zero gravity a concave variation of the butane with symmetry is present. As the residual-gravity level increases to 1 μg and to

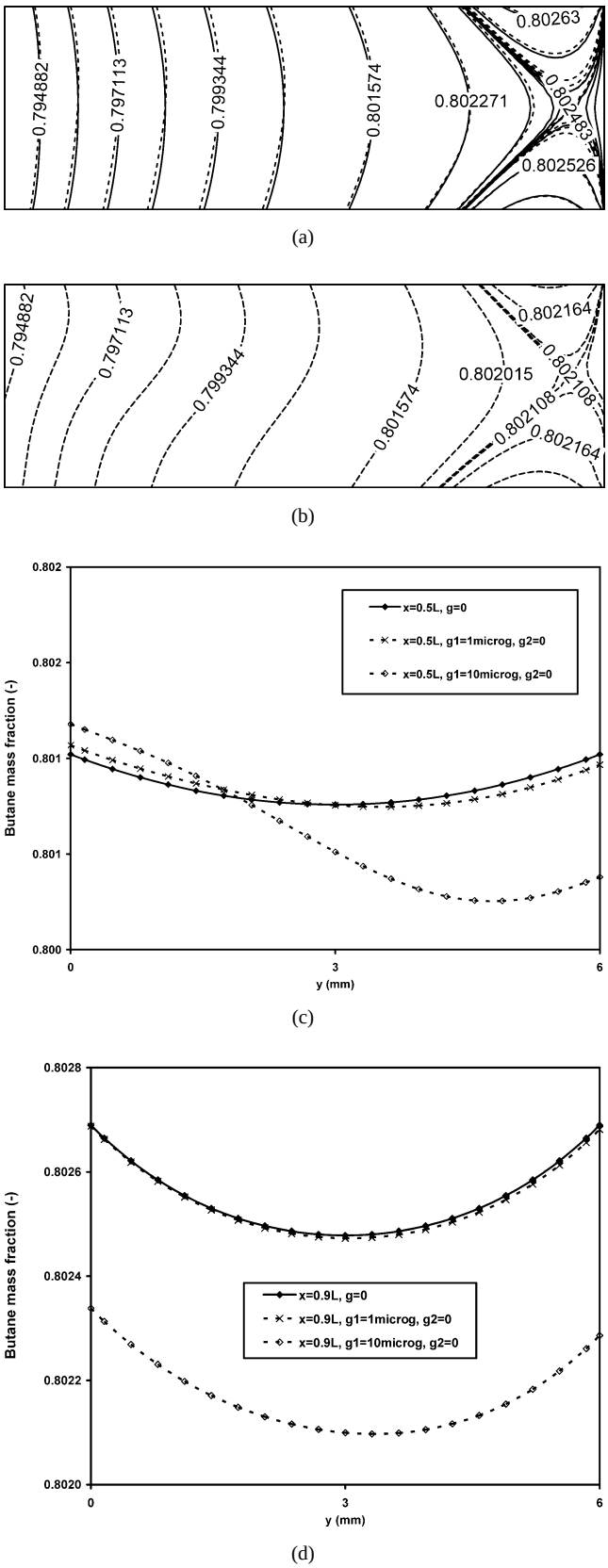

Fig. 4. Butane distributions in the cavity for different residual gravity conditions. (a) (- - - 1 μg, — zero gravity); (b) 10 μg condition; (c) Butane variation at the middle of the cavity ($x = 0.5$ L); (d) Butane variation near the cold wall at $x = 0.9$ L.

10 μg, the buoyancy convection becomes more dominant and a deformed butane profile indicates the effect that buoyancy convection has on the solutal diffusion in the cavity. Fig. 4(d) presents the butane distribution in the vertical direction near the cold end of the cavity. As the residual gravity increases, buoyancy effect reduces the butane diffusion toward the cold wall. However, the disturbances measured by the nonsymmetrical lateral butane distribution are more pronounced in the middle of the cavity as was shown in Fig. 4(c) than near the cold wall as presented in Fig. 4(d). The weaker butane differentiation due to increased residual gravity level yields a smaller Soret coefficient which is in agreement with the observations presented by Savino [14].

4.3. Influence of the g-jitter

Since the gravity vector used in our model has two components, after having studied the influence of the constant component (residual-gravity) we are going to focus on the time varying component characterised by its amplitude and frequency. In this section we will present the effect that the amplitude and the frequency will have on the mass distribution in the cavity. In each case, the time step, Δt, is obtained from the relation

$$\Delta t = (n_T + 1) \times T_{\text{jitter}}/8 \tag{13}$$

where n_T is a selected (integer) number of the vibration period, T_{jitter}. Thus by choosing the number of periods n_T greater than zero, we are able to reduce the computational time while maintaining the "same" periodic excitation over the system.

4.3.1. Effects of the amplitude variation on mass diffusion

Three different amplitude values varying between 10 and 100 μg will be analysed for this case. Fig. 5(a) presents the butane variation at P1 located near the hot wall. A comparison is made with the ideal condition of zero gravity. In this case as discussed earlier, a decrease in butane concentration near the hot wall is evident with time thus the butane migrates towards the cold wall. A stable oscillating regime is obtained for the three amplitudes of the g-jitter. Considering the 10 μg-amplitude g-jitter with no residual gravity, for example, the butane concentration oscillates at the same frequency as the original excitation of 0.01 Hz ($n_T = 40$). As the amplitude of the g-jitter increases, the oscillation amplitude changes very slightly while the difference between the initial value and the average value of the concentration is significantly reduced. Increasing the amplitude on the g-jitter enhances the mixing of the fluid in the cavity and therefore reduces species differentiation. The velocity in the x-direction as presented in Fig. 5(b) is also strongly affected by the amplitude variation. Although the velocity magnitude is small—strictly speaking—, nevertheless it is important for a diffusion case as the one presented in this paper. This large oscillation will definitely enhance the mixing in the fluid cavity therefore

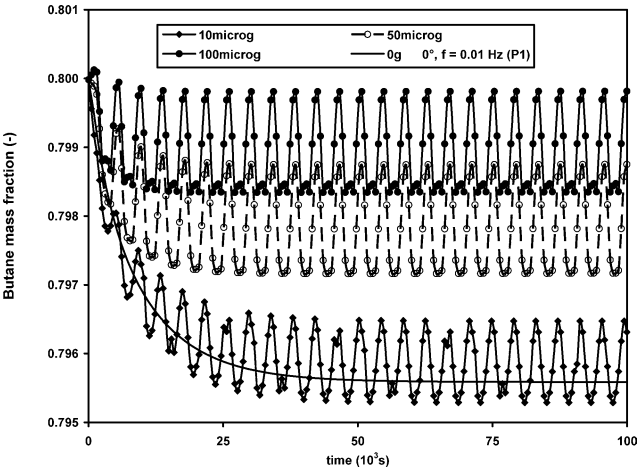

(a)

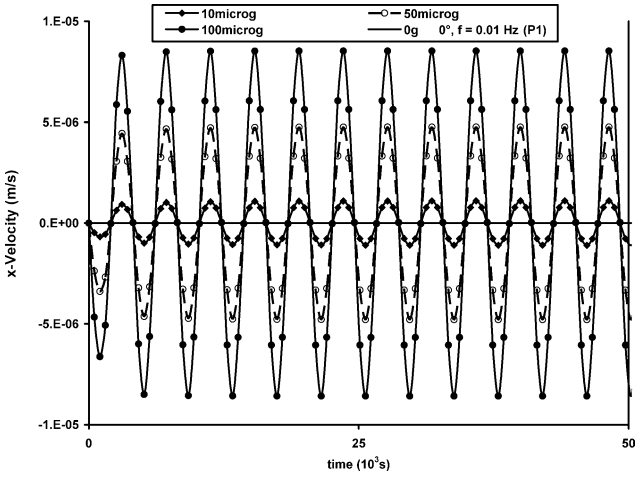

(b)

Fig. 5. Butane and velocity variation near the hot wall. (a) Butane distribution near the hot wall; (b) Horizontal velocity component near the hot wall.

defeating the purpose of measuring the thermal and species diffusion coefficient in the g-jitter environment.

Another important parameter to study is the ratio of thermal diffusion coefficient D^T to the species diffusion coefficient D^c known as the Soret coefficient. Fig. 6 presents the variation of the Soret at P1 near the hot wall. As one can see a large fluctuation of the Soret coefficient is another indication of the importance of taking varying thermal and species diffusion coefficient into account during the computation. Such observation was also identical for the two other points P2 and P3, which are located at the middle and near the cold end of the cavity. The Soret coefficient decreases with increasing amplitude of the g-jitter as a consequence of reduced species gradient in the cavity.

4.3.2. Frequency variation effect on mass diffusion

In the previous section we highlighted the importance the amplitude will have on the mass diffusion as well as on the Soret coefficient. In the present case, the amplitude was maintained constant at 10 μg and the frequency was

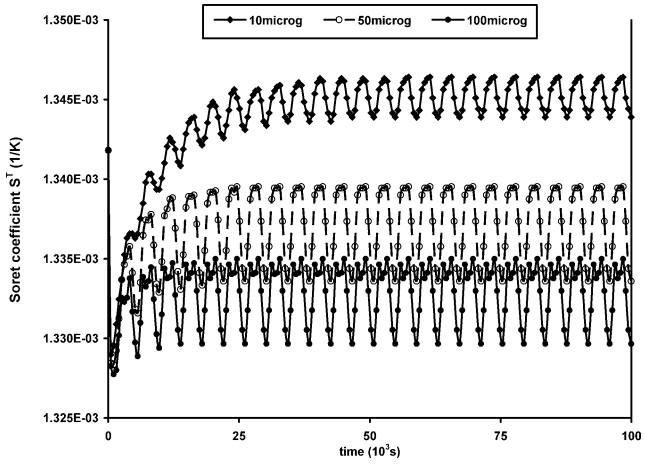

Fig. 6. Soret number variation near the hot wall for different jittering amplitudes.

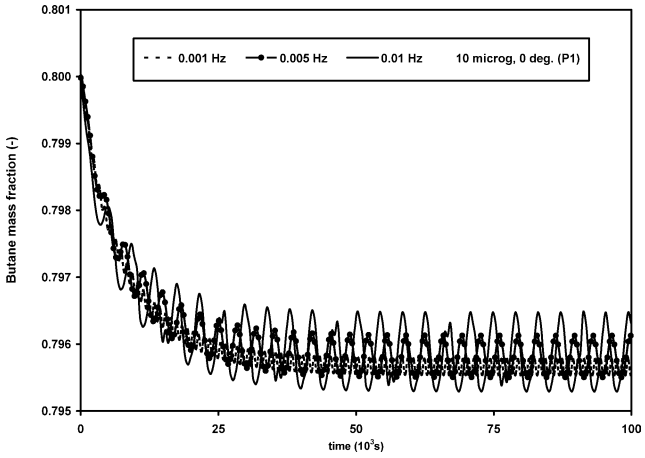

Fig. 7. Butane variations near the hot wall for different jittering frequencies.

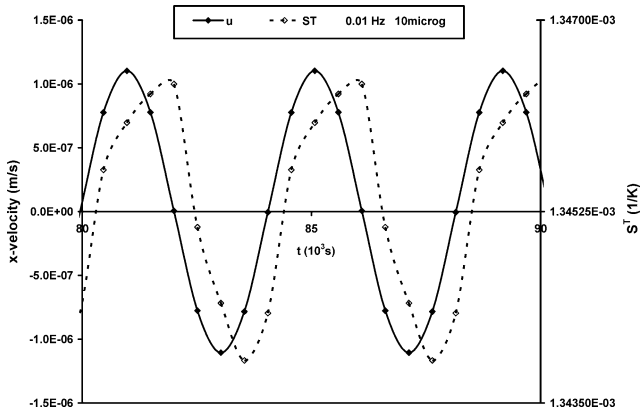

Fig. 8. Flow and Soret coefficient at 0.01 Hz (amplitude = 10 μg).

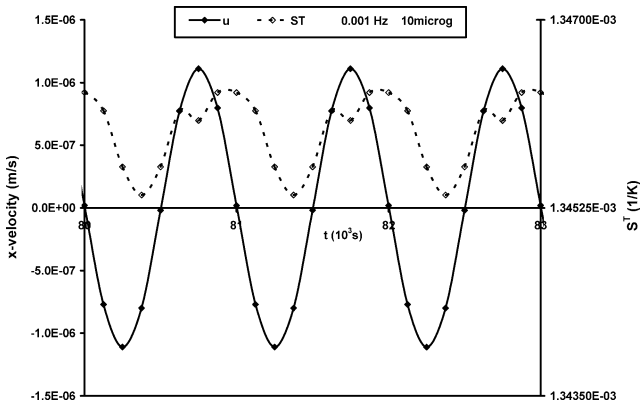

Fig. 9. Flow and Soret coefficient for 0.001 Hz (amplitude = 10 μg).

the varying parameter in the gravity vector. Because we are interested in low frequency condition, which does exist in the frequency spectrum on board the International Space Station, three different frequencies of 0.001, 0.005 and 0.01 Hz will be used in this model, with n_T equal 0, 16 and 40, respectively, for the calculation of corresponding time steps. Fig. 7 presents the variation of the butane at point P1 near the hot wall. It is evident to observe that even with a low frequency of 0.001 Hz ($n_T = 0$) the mass diffusion is affected with the gravity oscillation; with more pronounced effect at a higher frequency. The amplitude of fluctuations of the butane concentration increases with the frequency, with a slight change in the average value. The Soret coefficient oscillates due to the external disturbances. As the frequency is decreasing from 0.01 to 0.001 Hz, the Soret coefficient variation is decreasing accordingly and is reaching the variation which could be obtained for the zero gravity condition.

In order to better examine the variation of the Soret and the velocity for a short period of time, Figs. 8 and 9 presents those variations. In Fig. 8 the Soret coefficient as well as the velocity in the horizontal direction is presented. The time step that was used to get the results shown on Fig. 8 is $41 \times T_{\text{jitter}}/8$ (T_{jitter} is the period of oscillation of the g-jitter); thus $n_T = 40$. It is evident that the flow manifests a sinusoidal variation with a frequency identical to the excitation frequency of 0.01 Hz; however, the Soret coefficient oscillates at the same frequency but with a phase shift and the variation is not sinusoidal. This behaviour of the Soret coefficient is explained by the fact that the flow characteristic time is smaller than the mass diffusion characteristic time. The nonsinusoidal shape of the Soret coefficient may be attributed to the buoyancy convection disturbing the mass diffusion for a time interval.

Fig. 8 is repeated but for the lower frequency of 0.001 Hz as shown in Fig. 9. Here the time step (or time interval) was $T_{\text{jitter}}/8$. The flow variation is identical in shape to the previous case. However, the Soret coefficient profile is not purely sinusoidal. First the Soret coefficient amplitude of variation in value has been reduced due to the low frequency and secondly, the mass characteristic time is smaller making the flow disturbances more obvious in this case. The Soret coefficient tends to oscillate but with the back flow, this oscillation is distorted.

5. Conclusion

In this paper we have studied the effect the time dependent gravity vector will have on the mass diffusion in a binary fluid mixture. In the earth gravity condition, a constant butane distribution in the fluid mixture is due to the mixing generated by the strong buoyancy convection. Soret effect was not very apparent in this case. For the zero gravity condition, it was found that mass diffusion is important with butane being the heavy component of the mixture migrating to the cold wall due to the Soret effect. As the gravity vector became time dependent it was found that with a variation of amplitude and frequency, the vibration affects the mass diffusion. Finally we have shown for the first time that even the Soret number which is the ratio of the thermal diffusion to the species diffusion oscillates with time at the same frequency as the original excitation. However, the backflow disturbs this variation and makes it nonsinusoidal in shape.

Acknowledgement

We acknowledge the financial support of the Canadian Space Agency (CSA) and the National Science and Engineering Research Council of Canada (NSERC).

References

[1] J.H. Merkin, Oscillatory free convection from an infinite horizontal cylinder, J. Fluid Mech. 30 (1967) 561.
[2] B.J. Davidson, Heat transfer from a vibrating circular cylinder, Internat. J. Heat Mass Transfer 16 (1973) 1703.
[3] E.W. Haddon, N. Riley, The heat transfer between concentric vibrating circular cylinders, Q.J. Mech. Appl. Math. 34 (1981) 345.
[4] D.A.S. Rees, I. Pop, The effect of g-jitter on vertical free convection boundary-layer flow in porous media, Internat. Comm. Heat Mass Transfer 27 (2000) 415.
[5] D.A.S. Rees, I. Pop, The effect of g-jitter on free convection near a stagnation point in a porous medium, Internat. J. Heat Mass Transfer 44 (2001) 877.
[6] T.C. Jue, B. Ramaswamy, Numerical analysis of thermosolutal flows in a cavity with gravity modulation effects, Heat Mass Transfer 38 (2002) 665.
[7] R. Monti, R. Savino, A new approach to g-level tolerability for fluid and material science experiments, Acta Astronautica 37 (1995) 313.
[8] R. Savino, R. Monti, M. Piccirillo, Thermovibrational convection in a fluid cell, Comput. Fluids 27 (1998) 923.
[9] R.W. Smith, The influence of g-jitter on liquid diffusion—The QUELD/MIM/MIR Programme, Microgravity Sci. Technol. 11 (2) (1998) 78.
[10] R. Savino, R. Monti, Convection induced by residual-g and g-jitters in diffusion experiments, Internat. J. Heat Mass Transfer 42 (1999) 111.
[11] G.Z. Gershuni, A.K. Kolesnikov, J.C. Legros, B.L. Myznikova, On the vibrational convective instability of a horizontal binary-mixture layer with soret effect, J. Fluid Mech. 330 (1997) 251.
[12] G.Z. Gershuni, A.K. Kolesnikov, J.C. Legros, B.L. Myznikova, On the convective instability of a horizontal binary-mixture layer with soret effect under transversal high frequency vibration, Internat. J. Heat Mass Transfer 42 (1999) 547.
[13] R. Monti, R. Savino, M. Lappa, On the convective disturbances induced by g-jitter on the space station, Acta Astronautica 48 (2001) 603.
[14] R. Savino, Residual-g and g-jitter effects on the measurement of the thermophysical properties in microgravity, Adv. Space Res. 29 (2002) 559.
[15] M. Chacha, D. Faruque, M.Z. Saghir, J.C. Legros, Solutal thermodiffusion in binary mixture in the presence of g-jitter, Internat. J. Thermal Sci. 41 (2002) 899.
[16] S.R. de Groot, P. Mazur, Nonequilibrium Thermodynamics, Dover, New York, 1984.
[17] K. Shukla, A. Firoozabadi, A new model of thermal coefficients in binary hydrocarbon mixtures, Indust. Engrg. Chem. Res. 37 (1998) 3331.
[18] A. Firoozabadi, Thermodynamics of Hydrocarbon Reservoirs, McGraw-Hill, New York, 1999.
[19] J.A. Jossi, L.I. Stiel, G. Thodos, The viscosity of pure substances in the dense gaseous and liquid phases, AIChE J. 8 (1962) 59.
[20] J. Lohrenz, B.G. Bray, C. Clark, Calculating viscosities of reservoir fluids from their compositions, JPT (1964) 1171.
[21] D.Y. Peng, D.B. Robinson, A new two-constant equation of state, Indust. Engrg. Chem. Fund. 15 (1976) 58.
[22] Ph. Georis, F. Montel, S. Van Vaerenbergh, Y. Decroly, J.C. Legros, Measurement of the soret coefficient in crude oil, SPE 50573 (1998) 57.
[23] S.V. Patankar, Numerical Heat Transfer and Fluid Flow, McGraw-Hill, New York, 1980.
[24] M. Chacha, M.Z. Saghir, S. Van Vaerenbergh, J.C. Legros, Influence of thermal boundary conditions on double-diffusive process in a binary mixture, Philosophical Magazine 83 (2003) 2109.